Reactions of C_2H_5 Radicals with O, O_3, and NO_3: Decomposition Pathways of the Intermediate C_2H_5O Radical

K. Hoyermann,*,† M. Olzmann,‡ J. Seeba,† and B. Viskolcz‡,§

Institut für Physikalische Chemie der Universität Göttingen, Tammannstr. 6, D-37077 Göttingen, Germany, and Institut für Physikalische Chemie der Universität Halle-Wittenberg, FB Chemie Merseburg, D-06099 Halle, Germany

Received: January 5, 1999; In Final Form: May 21, 1999

The reactions of C_2H_5 with O, O_3, and NO_3 have been investigated in a discharge flow reactor at room temperature and pressures between 1 and 3 mbar. The reaction products were detected by mass spectrometry with electron-impact ionization. The product pattern observed is explained in terms of the decomposition of an intermediately formed, chemically activated ethoxy radical. It is shown that, with this assumption, the experimentally determined branching ratios of the different product channels can be reproduced nearly quantitatively by RRKM calculations based on ab initio results for the stationary points of the potential energy surface of C_2H_5O. For $C_2H_5 + O$ and $C_2H_5 + O_3$, the existence of an additional, parallel channel leading to OH has to be assumed. High-pressure Arrhenius parameters for the unimolecular reactions of the ethoxy radical are given and discussed.

1. Introduction

Alkoxy radicals are important species in the atmospheric degradation of hydrocarbons as well as in combustion processes. Additionally, they play a crucial role in the pyrolysis of oxygen-containing hydrocarbons. Their chemistry and kinetics have been reviewed recently.[1] Among them, the ethoxy radical is of special interest because it is the least complex radical of this type that bears a C−C bond. Thus, besides the intrinsic interest in its kinetics, it may also serve as a prototype for gaining a first insight into the branching behavior of the higher oxy radicals.

A direct way to generate ethoxy radicals is the reaction

$$C_2H_5 + O \rightarrow C_2H_5O^* \quad (1)$$

In this case, one obtains C_2H_5O with an excess energy (indicated here and in the following by *) of about 390 kJ mol^{-1}. These highly excited radicals may undergo a variety of consecutive processes, the most important of which are

$$C_2H_5O^* \rightarrow CH_3 + HCHO \quad (2)$$

$$C_2H_5O^* \rightarrow H + CH_3CHO \quad (3)$$

$$C_2H_5O^* \rightarrow CH_3CHOH \quad (4)$$

and

$$C_2H_5O^* \rightarrow CH_2CH_2OH \quad (5)$$

Slagle et al.[2] determined a rate coefficient of 1.3×10^{14} cm^3 mol^{-1} s^{-1} for the reaction $C_2H_5 + O$ and relative branching fractions of 0.32 ± 0.06 for channel 2 and 0.40 ± 0.04 for channel 3. Furthermore, a path leading to $C_2H_4 + OH$ was observed, which contributes with a fraction of 0.23 ± 0.07.

In the present work, besides $C_2H_5 + O$, the reactions

$$C_2H_5 + O_3 \rightarrow \text{products} \quad (6)$$

and

$$C_2H_5 + NO_3 \rightarrow \text{products} \quad (7)$$

are investigated, and also preliminary experimental results[3] for the reaction

$$C_2H_5 + NO_2 \rightarrow \text{products} \quad (8)$$

are included in the discussion. The appearance of the same products in each case suggests that the processes considered may have in common an intermediately formed ethoxy radical, which subsequently decomposes. It carries a different amount of internal energy, depending on its method of formation. A further support for this hypothesis, at least for the reaction $C_2H_5 + NO_3$, comes from a recent work of Biggs et al.,[4] who directly detected C_2H_5O radicals in this system by laser-induced fluorescence. In an analogous way, we already interpreted the unimolecular reactions of differently generated benzoxy radicals,[5] and a similar approach was also used to describe the kinetic behavior of certain oxy radicals under atmospheric conditions.[6,7]

Thus, the present study has two objectives, which are interconnected. The first one is to obtain information on the mechanisms of reactions 6−8 by comparing them with the reaction $C_2H_5 + O$. Second, the experimental measurement of the branching ratios and their verification by statistical rate theory based on ab initio results is expected to offer a reliable access to the specific rate coefficients for the unimolecular reaction channels of C_2H_5O. The latter plays a key role for the temperature dependence of the C_2H_5O decomposition as well

* To whom correspondence should be addressed.
† Universität Göttingen.
‡ Universität Halle-Wittenberg.
§ Present address: Institut für Physikalische Chemie und Elektrochemie, Universität Karlsruhe, Kaiserstr. 12, D-76128 Karlsruhe, Germany.

10.1021/jp9900436 CCC: $18.00
Published on Web 07/02/1999

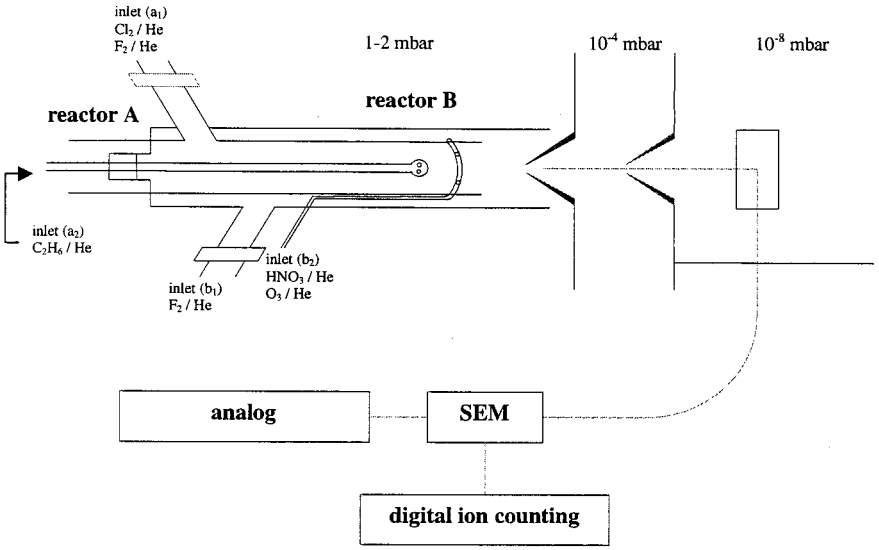

Figure 1. Experimental arrangement. For explanations see text.

as for the branching pattern of thermally or chemically activated ethoxy radicals under atmospheric or combustion conditions.

2. Experimental Section

Experimental Setup. The investigations were performed using an arrangement of discharge fast flow reactors coupled to a mass spectrometer by means of a molecular beam sampling device. The complete setup is shown schematically in Figure 1. Because the details of this setup and the procedures applied have been published previously (see, for example, ref 8), only a brief summary is given here.

The apparatus consists of two concentric reactors, A and B (Pyrex glass, inner diameter of 20 and 36 mm, respectively), which are movable with respect to each other. Reactor A, which additionally contains a movable inlet probe, serves as the source for the C_2H_5 radicals. They are produced by the reaction $C_2H_6 + X \rightarrow C_2H_5 + HX$ with X being optionally F or Cl. The halogen atoms are formed in a microwave discharge from highly diluted Cl_2/He and F_2/He mixtures (inlet a_1). They are mixed with the flow of C_2H_6/He injected by the movable inlet probe a_2.

The second set of reactants O, O_3, and NO_3 is supplied by the outer flow reactor B. The oxygen atoms are generated by a microwave discharge in O_2/He mixtures near inlet b_1. Ozone is directly added via inlet b_1 or b_2 as an O_3/He mixture. It is obtained, free of O_2, by means of a commercial ozonizer and collected in a cold trap by adsorption on silica gel. It was carefully degassed before use. The NO_3 radicals are generated,[5,9] free of NO_2, by the reaction of F atoms (inlet b_1) with HNO_3 admixed via inlet b_2.

The total length of the flow tube is 67 cm, and the reaction time can be varied by changing the relative position of the reactors and/or the linear flow velocity ($10-40$ m s^{-1}). Samples are withdrawn continuously, and the molecular beam, after being formed from nozzle and skimmer, crosses the electron impact ion source of a magnetic deflection type mass spectrometer. The energy of the ionizing electrons can be chosen from 4.5 to 29 eV to reduce ion fragmentation and to allow for a specific detection of labile and stable species at their parent peak or by a favorable fragmentation pattern. A high sensitivity is achieved by a phase-sensitive single ion counting technique. The microwave discharges are switched on and off, which corresponds to the presence and absence, respectively, of C_2H_5 radicals, O atoms, and NO_3 radicals. A two-channel counter is gated accordingly such that the sampling conditions are "reaction on" and "reaction off, background".

The concentrations of the stable reactants are regulated by mass-flow controllers and needle valves, respectively, where the needle valves were calibrated by following the pressure rise with time in a known volume. The concentrations of the labile species are determined by titration reactions and mass balances, C_2H_5 radicals, for example, by the consumption of a known flow of C_2H_6 by F or Cl atoms according to $C_2H_6 + X \rightarrow C_2H_5 + HX$ with $-\Delta[C_2H_6] = +\Delta[C_2H_5]$.

The chemicals used were of commercial grade (He, ≥99.996%; He/F_2 and F_2, ≥99.9%; He/Cl_2 and Cl_2, ≥99.8%; Ar, ≥99.6%, Messer-Griesheim; C_2H_6, ≥99.95%, Linde; CH_4, ≥99.995%, Merck-Schuchardt; HNO_3 (65% in H_2O); H_2SO_4 (95−98% in H_2O), Merck).

Experimental Results. The rationale of the experimental determination of the branching fractions for the title reactions using the product yields is as follows. (i) An unambiguous identification of the primary products was achieved by mass spectrometry at low ionization energies, which leads to a reduction of the ion fragmentation. The ionization energy was adjusted to greatly reduce mass interferences between parent mass peaks and those of fragment ions, e.g., $m/e = 29$ for $C_2H_5^+$ (C_2H_5 radical) and HCO^+ (fragment ion of $HCHO^+$), to allow for a reliable background subtraction, where direct mass interference exists (e.g., $m/e = 30$ for $C_2H_6^+$ and $HCHO^+$), and finally, to ensure an optimum signal-to-noise ratio. (ii) The product yields of the reactions $C_2H_5 + O_3$ and $C_2H_5 + NO_3$ were measured relative to that of the reaction $C_2H_5 + O$ by an immediate and repeated switching between the oxidizers O_3 and O, and NO_3 and O, respectively. (iii) Absolute product yields were obtained by adopting the branching fractions for $C_2H_5 + O$ from the detailed study of Slagle et al.[2] and our own reinvestigation.

The general procedure is illustrated qualitatively by Figure 2 for $C_2H_5 + O_3$. The spectra were recorded at a pressure of 1.7 mbar and a temperature of 300 K in the flow tube for a reaction time of 1.7 ms and with the initial concentrations $[O_3]_0 = 2 \times 10^{-11}$ mol cm^{-3} and $[C_2H_5]_0 = 4 \times 10^{-12}$ mol cm^{-3}. The ionization energy was 19.1 eV. In the absence of any oxidizer, the mass spectrum (Figure 2c) shows signals of the species C_2H_6 ($m/e = 30, 29, 28$), C_2H_5 ($m/e = 29, 28$), and

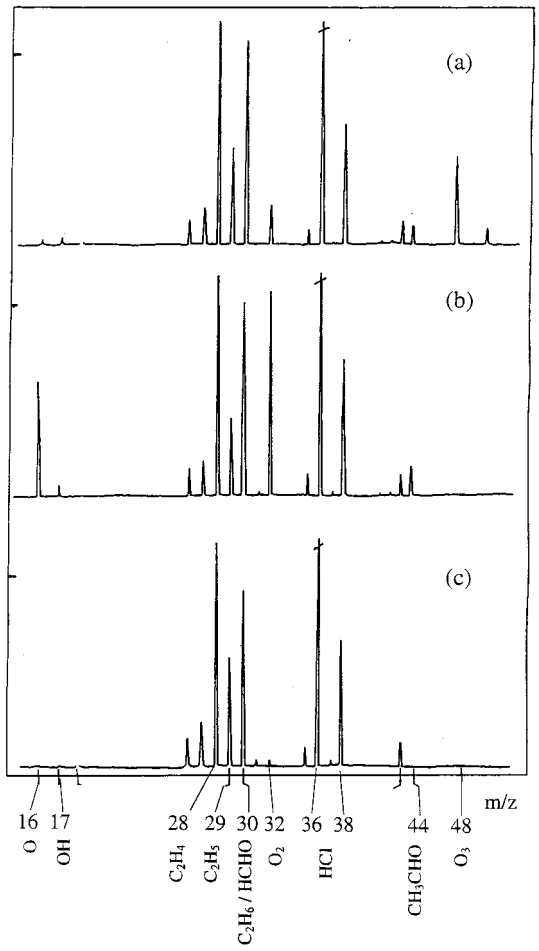

Figure 2. Mass spectra characterizing the product formation of the reactions $C_2H_5 + O_3$ (a) and $C_2H_5 + O$ (b) compared to the background spectrum (c). The latter was recorded with the reaction $C_2H_6 + Cl \rightarrow C_2H_5 + HCl$ being switched on, but under conditions where neither O_3 nor O (nor O_2) is present. For details, see text.

HCl ($m/e = 36$ and 38 for $H^{35}Cl$ and $H^{37}Cl$, respectively). Addition of O_3 leads to a signal increase at $m/e = 17$, 28, 30, and 44 due to the formation of OH, C_2H_4, HCHO, and CH_3CHO and a decrease at $m/e = 29$ due to the consumption of C_2H_5. Also, an increase at $m/e = 15$ due to the formation of CH_3 was observed but is not included in the sample spectra of Figure 2. No products are found at $m/e = 45$ (C_2H_5O) and $m/e = 77$ ($C_2H_5O_3$), whereas the formation of O_2 at $m/e = 32$ is accompanied by the consumption of O_3 at $m/e = 48$. Similar results are observed for the reaction $C_2H_5 + O$ (Figure 2b): formation of CH_3, OH, C_2H_4, HCHO, and CH_3CHO and the absence of C_2H_5O. Here, the mass peak $m/e = 16$ originates from O atoms and $m/e = 32$ from undissociated O_2/recombined O atoms. Quantitative product yields were obtained by following the product increase and the C_2H_5 consumption with time by single-ion counting at various distances between the reactant inlets and the sampling nozzle (cf. Figure 1). On the basis of the product yields of the calibration reaction, $C_2H_5 + O$,[2] mentioned above, our findings for the relative branching fractions are

$$\begin{aligned} C_2H_5 + O_3 &\rightarrow CH_3 + HCHO + O_2 \qquad 0.50 \pm 0.10 \\ &\rightarrow H + CH_3CHO + O_2 \qquad 0.30 \pm 0.06 \\ &\rightarrow C_2H_4 + OH + O_2 \qquad 0.19 \pm 0.08 \end{aligned}$$

The given errors result from the statistical error of the measurements (1 standard deviation) and the quoted errors of the reference reaction. These branching fractions are thought to be reliable, since they are derived from the temporal product profiles (i.e., minimizing the effects of adsorbed aldehydes at the reactor wall) and at low consumption (below 20%) of the C_2H_5 radicals (i.e., suppressing secondary reactions). Secondary reactions of the CH_3 radicals to be considered are $CH_3 + O_3 \rightarrow HCHO + H + O_2$ and $CH_3 + O \rightarrow HCHO + H$. Because these reactions are slower than the primary reactions (eqs 6 and 1) by a factor of 10 and 2, respectively, and because the consumption of C_2H_5 was kept low, they only negligibly alter the product distribution. The same holds for consecutive reactions caused by H atoms. This has been tested by a simulation of the product profiles, assuming the following mechanism with the given rate coefficients (in $cm^3\ mol^{-1}\ s^{-1}$): $k(C_2H_5 + O_3) = 1.5 \times 10^{13}$, ref 10; $C_2H_5 + O_3 \rightarrow H + CH_3CHO$, relative yield of 30%, this work; $H + O_3 \rightarrow OH + O_2$, $k = 1.7 \times 10^{13}$, ref 11; $H + C_2H_5 \rightarrow 2CH_3$, $k = 1.1 \times 10^{14}$, ref 12. For conversions of C_2H_5 below 20%, the influence of secondary reactions on the product distribution is well within the combined error margins of the measurements and the yields of the calibration reaction.

Reaction 7, $C_2H_5 + NO_3$, was studied in a manner analogous to that of reaction 6 with the following conditions: pressure, 2.5 mbar; temperature, 300 K; reaction times, 1−2.8 ms; initial concentrations $[NO_3]_0 = 2 \times 10^{-10}$ mol cm^{-3}, $[C_2H_5]_0 = (0.2-0.9) \times 10^{-10}$ mol cm^{-3} with $[HNO_3]_0/[F]_0 > 10$; ionization energy, 17 eV. The consumption of C_2H_5 corresponded to the formation of HCHO and CH_3CHO. No signals or significant signal increases were found at $m/e = 91$ ($C_2H_5ONO_2$), 45 (C_2H_5O), 47 (HNO_2), 63 (HNO_3), 28 (C_2H_4), and 17 (OH). The relative yields of HCHO and CH_3CHO as formed in reactions 7 and 1 were measured alternately and normalized to the consumption of the C_2H_5 radicals. When the quoted branching fractions for $C_2H_5 + O$ are employed, the following values for reaction 7 were found:

$$\begin{aligned} C_2H_5 + NO_3 &\rightarrow CH_3 + HCHO + NO_2 \qquad 0.88 \pm 0.15 \\ &\rightarrow H + CH_3CHO + NO_2 \qquad 0.25 \pm 0.10 \end{aligned}$$

The derived total product yield of 1.13 ± 0.18 indicates the absence of further reaction channels. The influence of secondary reactions has been tested too, assuming the following mechanism with the given rate coefficients (in $cm^3\ mol^{-1}\ s^{-1}$): $C_2H_5 + NO_3$, $k = 2.7 \times 10^{13}$, ref 4; $H + NO_2 \rightarrow OH + NO$, $k = 8.4 \times 10^{13}$, ref 13; $H + C_2H_5 \rightarrow 2CH_3$, $k = 1.1 \times 10^{14}$, ref 12; $CH_3 + NO_2$, $k = 1.4 \times 10^{13}$, ref 14. It turns out that no significant corrections to our primary data have to be applied.

The products of the reaction $C_2H_5 + O$ were studied in the flow reactor by their temporal increase within known reaction times. Several calibrations have been performed. The consumption of C_2H_5 and the formation of CH_3 were made quantitative by the mass spectrometric calibration of the C_2H_5 and CH_3 signals. This was accomplished by employing the reactions $C_2H_6 + F \rightarrow C_2H_5 + HF$ and $CH_4 + F \rightarrow CH_3 + HF$; a constant F atom flow was titrated either by C_2H_6 or by CH_4 (inlet a_2 in Figure 1). The mass spectrometric sensitivity of HCHO and its ion fragmentation pattern at $m/e = 30$ and 29 were determined by studying the reaction $CH_3 + O \rightarrow HCHO + H$. Because a second channel, $CH_3 + O \rightarrow CO + H_2 + H$, with an efficiency of 40% is discussed in the literature,[15] this uncertainty can enter into the absolute calibration of HCHO. Acetaldehyde was calibrated directly using a liquid sample.

Apart from the mass spectrometric investigation, the formation of OH has been studied additionally by means of a flash

photolysis/OH-LIF arrangement. In situ photolysis of C_2H_5I/SO_2 mixtures was employed for the generation of C_2H_5 radicals and O atoms. The time-resolved observation of the formation of OH in different vibrational levels reveals a nonthermal distribution for $v = 0$, 1, and 2.[16] A similar nonequilibrium distribution for OH ($v = 1$, ..., 5) from $C_2H_5 + O$ has also been found in a very recent investigation by Lindner et al.,[17] using IR chemiluminescence for detection.

For $C_2H_5 + O$, our experiments in the flow reactor lead essentially (within 20%) to the same branching fractions as reported by Slagle et al.[2] This is in some contrast to a former study in our laboratory,[18] where the determination of the product yields relied mainly on the cracking pattern of aldehydes from high-resolution mass spectra at a high ionization energy (70 eV). A low-pressure expansion reactor with poor residence-time control was used. Since the present alternative procedure is based on the direct observation of the products together with their temporal profile and on the direct control of the reaction time in the flow reactor, we favor the new results. On account of the high-quality measurement of Slagle et al.,[2] we adopted their values as our standard.

3. Theoretical Analysis of the Branching Fractions

Molecular Distribution Functions. For our experimental conditions, the quantities of interest that govern the branching ratios can be defined as low-pressure limiting rate coefficients for the different chemically activated unimolecular reactions of the ethoxy radical (see, for example, refs 19−21). For each reaction pathway j

$$k_{0j} = \int_{E_{0,\min}}^{\infty} k_j(E)\, F^{ss}(E)\, \mathrm{d}E \tag{9}$$

with the normalized steady-state distribution

$$F^{ss}(E) = \frac{F(E)}{\sum_i k_i(E)} \left[\int_{E_{0,\min}}^{\infty} \frac{F(E)\, \mathrm{d}E}{\sum_i k_i(E)} \right]^{-1} \tag{10}$$

and the corresponding specific rate coefficients $k_i(E)$. $E_{0,\min}$ denotes the lowest threshold energy among the different unimolecular channels i. For the nascent distribution of the ethoxy radicals, $F(E)$, one has to discriminate between two different cases.

First, if C_2H_5O is directly formed from $C_2H_5 + O$ via reaction 1,

$$F(E) = F'(E) \equiv \frac{W(E)\, \exp[-E/(k_B T)]}{\int_0^{\infty} W(E)\, \exp[-E/(k_B T)]\, \mathrm{d}E} \tag{11}$$

where k_B is Boltzmann's constant, T the temperature, and $W(E)$ the combined sum of states of C_2H_5 and O.[19] In our calculations, the latter was simply represented by the sum of states for C_2H_5, including the external rotations. One should note that the form of the distribution is not very sensitive with respect to the molecular parameters, and hence, this approach is quite sufficient.[19]

Second, in the other instances, the ethoxy radical is assumed to be formed by two consecutive reactions, namely,

$$C_2H_5 + XO \rightarrow C_2H_5XO^* \tag{12}$$

and

$$C_2H_5XO^* \rightarrow C_2H_5O^* + X \tag{13}$$

where XO stands for O_3, NO_3, and NO_2, respectively. In this case, the distribution of the intermediate $C_2H_5XO^*$ can be expressed by eq 11 with the correspondingly altered $W(E)$. Here, we take into account all internal and external rotational degrees of freedom of C_2H_5 and XO. Presumably, the decomposition of $C_2H_5XO^*$ proceeds statistically; the resulting distribution of $C_2H_5O^*$ for a well-defined disposable energy E' in $C_2H_5XO^*$ is[5,6,19,22]

$$P_{C_2H_5O}(E,E') = \frac{\rho_{C_2H_5O}(E)\, W_X(E'-E)}{\int_0^{E'} \rho_{C_2H_5O}(y)\, W_X(E'-y)\, \mathrm{d}y} \tag{14}$$

where ρ and W denote the density and sum of states, respectively, for the corresponding fragment, C_2H_5O or X. Finally, by allowing E' to be distributed according to eq 11, the combination of eqs 11 and 14 leads to

$$F(E) = \int_{\max(E,E^+)}^{\infty} P_{C_2H_5O}(E,E')\, F'(E')\, \mathrm{d}E' \tag{15}$$

where the sums of states in F' have to be altered as mentioned above and

$$E^+ = \Delta H_f^\circ(C_2H_5) + \Delta H_f^\circ(XO) - \Delta H_f^\circ(C_2H_5O) - \Delta H_f^\circ(X) \tag{16}$$

The quantity E^+, which follows from the heats of formation at 0 K, ΔH_f°, represents the minimum excess energy of C_2H_5-XO* above its threshold for the dissociation according to eq 13, and the definition after eq 16 presumes that reaction 12 and the reverse reaction of eq 13 are barrierless. The situation is illustrated in Figure 3. In this way, the intermediate $C_2H_5XO^*$ does not need to be characterized explicitly, and the only assumption is that its decomposition is fast compared to the collisional stabilization. Because, under our experimental conditions, the gas kinetic collision number is on the order of 10^7 s^{-1}, this should be surely the case for all of our systems, maybe with a certain exception for $C_2H_5NO_2^*$, which has the lowest value for E^+ (see below). But even in this case, the influence on the branching ratios can be neglected. For $C_2H_5NO_3^*$, Biggs et al.[4] estimated the collisional stabilization by a QRRK model and derived a fractional contribution below 0.03 even for a pressure as high as 1 atm. For our actual calculations, all enthalpies of formation in eq 16 have been taken from standard tables.[23,24] The resulting values for E^+ are 32 370, 23 480, 14 940, and 6780 cm^{-1} for reactions 1, 6, 7, and 8, respectively. The sums and densities of states were exactly counted[20,21,25,26] with molecular parameters from the following references: O_2, O_3, NO, and NO_2,[27] NO_3,[28,29] and C_2H_5.[30,31]

Specific Rate Coefficients. The specific rate coefficients for reactions 2−5 have been calculated by RRKM theory (ref 32; see also refs 19−21 and 26):

$$k_i(E) = \frac{W_i(E)}{h\, \rho_{C_2H_5O}(E)} \tag{17}$$

where h represents Planck's constant and W_i the sum of states of the transition state i. The molecular parameters required have been obtained by ab initio calculations. We employed the Gaussian 92 program suite[33] and calculated the structures and harmonic frequencies at the MP2/6-31G* level and the energies at the MP2/6-311+G** level. Recommended scaling factors of

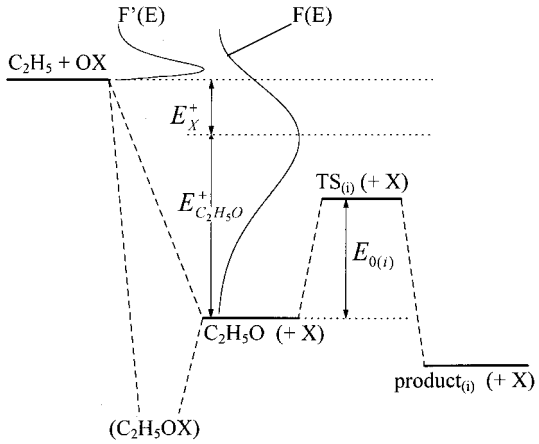

Figure 3. Schematic potential energy diagram for the reaction C_2H_5 + OX → $product_{(i)}$ + X. The energy E^+, representing the thermochemical limit from eqs 15 and 16, is shared between the two fragments, i.e., $E^+ = E^+_{C2H5O} + E^+_X$. The molecular populations $F'(E)$ and $F(E)$ are defined by eqs 11 and 15, respectively. The symbol $TS_{(i)}$ denotes the transition state for reaction i and $E_{0(i)}$ the corresponding threshold energy.

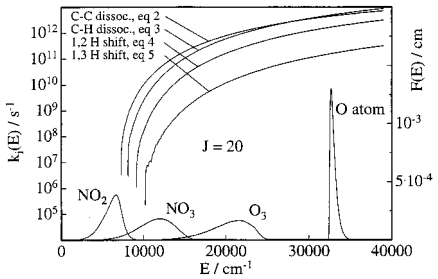

Figure 4. Specific rate coefficients for reactions 2−5 and nascent molecular distribution functions of $C_2H_5O^*$ for the different formation reactions. From low to high energies: C_2H_5 + NO_2, NO_3, O_3, and O, respectively.

0.9427 for the frequencies and 0.9646 for the zero-point energies have been used.[34] The results are shown in Table 1. Additionally, in view of a very recent experimental and theoretical study of the thermal decomposition of C_2H_5O,[35] we have examined the sensitivity of the branching fractions regarding variations in the threshold energies of the dissociation channels (eqs 2 and 3). The effects are discussed in the next section.

In calculating the sums and densities of states, angular momentum conservation was accounted for. From the experimental rate coefficients of reactions 1 and 6−8,[2,3,10,36−39] an orbital angular momentum due to the reactive collision can be derived.[40,41] One obtains values for the corresponding quantum number between 15 for C_2H_5 + O_3 and 25 for C_2H_5 + O. Considering the thermally averaged angular momenta of the reactants too and employing the triangle inequality, one finally estimates averaged total angular momentum quantum numbers $\langle J \rangle \approx 20$ (see, for example, refs 41−43). Thus, in what follows, all quantities discussed were calculated for the case $J = 20$. We also checked the cases $J = 0$ and $J = 50$ as reasonable lower and upper limits but found only very small influences on the branching ratios. In general, the energy is counted from the rovibrational ground state of C_2H_5O, and a step size of 10 cm^{-1} was used. Symmetry effects are taken into account by reaction path degeneracies, which are 1, 2, 2, and 1 for reactions 2, 3, 4, and 5, respectively. The somewhat unexpected value of 1 for the 1,3 H shift can be most easily envisaged by considering the three H atoms of the methyl group distinguishable. Then, by rotation around the C−C bond, three different configurations of both the radical and the transition state are accessible. Hence, the reaction path degeneracy is 1. For a detailed discussion of this topic see ref 21.

4. Results and Discussion

The computed specific rate coefficients and the nascent molecular distributions of C_2H_5O are shown in Figure 4. A comparison is made in Table 2 between the experimentally determined and calculated relative fractions for the different reaction channels. It can be seen that especially the branching between reaction 3 (H + CH_3CHO) and reaction 2 (CH_3 + HCHO) is very well reproduced by our calculations. The corresponding ratios k_{03}/k_{02} are 1.10 (1.25), 0.76 (0.6), and 0.33 (0.28) for the activating reactions C_2H_5 + O, O_3, and NO_3, respectively (experimental values in parentheses). In contrast to the calculations in ref 2, the predominance of reaction 3 over reaction 2 for C_2H_5 + O is correctly predicted by our model. Moreover, the decrease of the ratio to values below unity in going from the oxidant O via O_3 to NO_3 is also reproduced. This behavior can be understood by inspection of Figure 4; the curves of the specific rate coefficients for the C−C and the C−H bond dissociation cross at an energy located between the populations generated by C_2H_5 + O_3 and C_2H_5 + O. Whereas the C−C bond dissociation is the fastest reaction at low and moderate excitation, C−H bond breaking dominates at higher energies.

An alternative route, which may lead to CH_3CHO is the 1,2 H shift of the ethoxy radical, reaction 4, followed by a cleavage of the O−H bond in CH_3CHOH in competition with the isomerization back to C_2H_5O. As can be seen from Table 2, this channel might be relatively important. If it fully contributes to the CH_3CHO formation, i.e., if the reverse isomerization is completely neglected, then the predicted overall CH_3CHO yields would be 0.45 for C_2H_5 + O, 0.40 for C_2H_5 + O_3, and 0.27 for

TABLE 1: Calculated Potential Energies E_{pot}, Harmonic Wavenumbers ν_i (Scaled by 0.9427), Rotational Constants *A*, *B*, *C*, and Resulting Threshold Energies at 0 K, E_0, As Obtained from the Ab Initio Calculations[a]

	E_{pot}/E_h	ν_i, *A*, *B*, *C*/cm^{-1}	E_0/kJ mol^{-1}
C_2H_5O	−153.965 594	251, 374, 611, 879, 923, 967, 1103, 1227, 1297, 1370, 1458, 1476, 1515, 2896, 2947, 2949, 3038, 3047, 1.1608, 0.34610, 0.29675	
TS(2)	−153.928 270	649i, 170, 303, 558, 610, 700, 920, 1139, 1227, 1397, 1415, 1478, 1631, 2804, 2863, 3002, 3163, 3183, 1.1118, 0.27443, 0.24174	87.22
TS(3)	−153.920 922	1641i, 210, 463, 557, 627, 852, 912, 1092, 1167, 1355, 1375, 1448, 1452, 1633, 2798, 2938, 3023, 3056, 1.3655, 0.32308, 0.29608	96.67
TS(4)	−153.919 183	2135i, 188, 407, 619, 881, 891, 1053, 1091, 1155, 1334, 1382, 1449, 1462, 2465, 2921, 2976, 3001, 3035, 1.4775, 0.31008, 0.27915	109.51
TS(5)	−153.914 919	2273i, 368, 725, 807, 903, 980, 1069, 1083, 1108, 1189, 1249, 1401, 1503, 1692, 2952, 3013, 3020, 3131, 0.92657, 0.44723, 0.34284	121.67

[a] TS(*i*) represents the transition state for reaction *i*. (E_h = 2625.500 kJ mol^{-1})

TABLE 2: Measured and Calculated Relative Branching Fractions

	$C_2H_5 + O$			$C_2H_5 + O_3$		$C_2H_5 + NO_3$	
	exptl[a]	calcd	calcd[a]	exptl	calcd	exptl	calcd
$CH_3 + HCHO$	0.32 ± 0.06	0.31	0.56	0.50 ± 0.10	0.41	0.88 ± 0.15	0.73
$H + CH_3CHO$	0.40 ± 0.04	0.34	0.31	0.30 ± 0.06	0.31	0.25 ± 0.10	0.24
$OH + C_2H_4$	0.23 ± 0.07			0.19 ± 0.08			
1,3 H shift		0.02	0.02		0.01		0.001
1,2 H shift		0.11	0.11		0.09		0.03

[a] From ref 2. In our calculated values, the OH yields attributed to the direct channel (i.e., the fraction not formed via 1,3 H shift) are included in the balance.

$C_2H_5 + NO_3$ as is evident from Table 2. However, this is still in reasonable agreement with the experimental findings.

In contrast to this good agreement, the measured OH yield is poorly reproduced by our model. The pathway leading to $C_2H_4 + OH$ is the 1,3-isomerization of C_2H_5O, reaction 5, followed by a β-decomposition of the 2-hydroxyethyl radical. But, as was already discussed in ref 2, the rate of this isomerization is too low to account for the OH yields observed. As can be realized from Table 2, this channel only contributes with 2% in the case of $C_2H_5 + O$ and with 1% for $C_2H_5 + O_3$, whereas the experimental OH yields are 23% and 19%, respectively (cf. also Figure 4). Obviously, an additional route exists. Whether this is a direct metathesis or an additional reaction via a chemically activated intermediate remains an open question. Particularly for $C_2H_5 + O_3$, the latter cannot definitely be ruled out. A strong support, however, for a direct abstraction mechanism in the case of $C_2H_5 + O$ comes from recent measurements of the vibrational state distribution of the OH radicals formed. As already mentioned in section 2, a nonthermal distribution was detected in an IR chemiluminescence study by Lindner et al.[17] and in a laser-induced fluorescence investigation from our laboratory.[16] Such an inverted population is a strong indication of a direct abstraction mechanism.[44]

In a supplementary study, also the reaction $C_2H_5 + NO_2$ was investigated in a discharge−flow experiment.[3] However, dissociation products are difficult to assign in the mass spectrum. Only the relative fraction of the channel leading to $CH_3 + HCHO$ was estimated to be greater than (0.1 ± 0.05).[3] Because in this case the energy of the C_2H_5O population is comparatively low, the specific rate coefficients are on the order of the collision frequency (cf. Figure 4). Hence, the simple approach using eqs 9 and 10 is no longer adequate. To account for the influence of the collisions, we performed a master-equation analysis[19−21] with a simple stepladder model described elsewhere.[45] For step sizes of 100 and 500 cm^{-1}, which correspond to average energies transferred per collision of -20 and -370 cm^{-1} and which should embrace the reasonable range,[21,35,46] we obtained relative fractions for the decomposition of 0.19 and 0.15, respectively. This is essentially in agreement with the experimental result. From our calculation follows a branching ratio of 100 in favor of $CH_3 + HCHO$ over $H + CH_3CHO$, whereas reactions 4 and 5 are completely negligible. In view of the limited experimental information, a more detailed discussion is not indicated at this point. Nevertheless, the mechanism for this reaction seems to resemble those for the other systems investigated in this work.

Unfortunately, to date there is little information available on the kinetics of the thermal unimolecular reactions of C_2H_5O. In Table 3 some recently recommended values for the high-pressure Arrhenius parameters are compared with the results derived[19,20] from our ab initio data. The agreement with the recommendations based on the earlier experimental results (activation energies of ca. 90 kJ mol^{-1} for the C−C bond dissociation) is satisfactory.

TABLE 3: High-Pressure Arrhenius Parameters (Ab Initio Based Values for $T = 400$ K)

reaction	E_∞/kJ mol^{-1}	$\log(A_\infty/s^{-1})$	ref
2	90.4	15.0	47, 50
	90.4	13.7	48
	90.0	13.9	49, 36
	84.5	14.3	1a
	70.3	13.0	35
	91.9	13.9	this work
3	97.9	14.4	47
	100.6	13.8	this work
4	112.9	13.7	this work
5	123.3	12.9	this work

The somewhat lower value for E_∞ given by Atkinson[1a] follows from a reevaluation of the relative measurement from Batt and Milne.[47,50] As already mentioned above, also a very recent investigation[35] of the thermal decomposition of C_2H_5O favors a lower high-pressure limiting value for the activation energy compared to earlier studies. This is also supported by ab initio calculations on QCISD(T) and MP2 level with large basis sets including diffuse and high angular momentum functions.[35] Because in these calculations the threshold energies for both the C−C and the C−H bond dissociation are lowered by >10 kJ mol^{-1} compared to our MP2/6-311+G**//MP2/6-31G* results, the corresponding branching ratio is hardly influenced. This was carefully checked using the results from ref 35. The relative branching fractions obtained lie within the error margins of the experimental results given in Table 2.

It is obvious that the investigation of product yields can provide detailed information regarding the underlying mechanism and the relative position of the reaction thresholds but is necessarily less suited to precisely determine absolute barrier heights.

5. Conclusions

The experimental branching fractions under low-pressure conditions for the reactions of C_2H_5 with O, O_3, NO_3, and NO_2 can be explained by assuming the formation of an intermediary ethoxy radical, which subsequently decomposes. For $C_2H_5 + O$ and $C_2H_5 + O_3$, an additional, parallel pathway leading to OH is likely to exist. In the case of $C_2H_5 + O$ this is probably a direct abstraction channel with a relative contribution of ca. 20%. For the unimolecular reactions of C_2H_5O, an RRKM description based on ab initio results for the stationary points of the potential energy surface provides a nearly quantitative agreement with the experimental findings. No adjustable parameters are required. Thus, the calculated molecular and transition-state data in connection with reliable values for the threshold energies can be used to calculate the specific rate coefficients for the different unimolecular reaction channels of the ethoxy radical. These values can be used for a detailed modeling of the C_2H_5O kinetics in atmospheric or combustion systems.

Acknowledgment. The authors thank Dr. C. Fittschen and Prof. H. Hippler for valuable discussions and for providing results of their work prior to publication. M.O. thanks Prof. K. Scherzer for continuous support. Funding by the Deutsche Forschungsgemeinschaft (SFB 357 "Molekulare Mechanismen Unimolekularer Prozesse") and the Fonds der Chemischen Industrie is gratefully acknowledged. The ab initio calculations were carried out at the Regionales Rechenzentrum für Niedersachsen Hannover.

References and Notes

(1) (a) Atkinson, R. *Int. J. Chem. Kinet.* **1997**, *29*, 99. (b) Heicklen, J. *Adv. Photochem.* **1988**, *14*, 177.

(2) Slagle, I. R.; Sarzyński, D.; Gutman, D.; Miller, J. A.; Melius, C. F. *J. Chem. Soc., Faraday Trans. 2* **1988**, *84*, 491.

(3) Rohde, G. Ph.D. Dissertation, Göttingen, 1991.

(4) Biggs, P.; Canosa-Mas, C. E.; Fracheboud, J.-M.; Shallcross, D. E.; Wayne, R. P. *J. Chem. Soc., Faraday Trans.* **1995**, *91*, 817.

(5) Hoyermann, K.; Seeba, J.; Olzmann, M.; Viskolcz. B. *Ber. Bunsen-Ges. Phys. Chem.* **1997**, *101*, 538.

(6) Orlando, J. J.; Tyndall, G. S.; Bilde, M.; Ferronato, C.; Wallington, T. J.; Vereecken, L.; Peeters, J. *J. Phys. Chem. A* **1998**, *102*, 8116.

(7) Schneider, W. F.; Wallington, T. J.; Barker, J. R.; Stahlberg, E. A. *Ber. Bunsen-Ges. Phys. Chem.* **1998**, *102*, 1850.

(8) Bartels, M.; Edelbüttel-Einhaus, J.; Hoyermann, K. *22nd Symposium (International) on Combustion*; The Combustion Institute: Pittsburgh, PA, 1988; p 1041.

(9) Becker, E.; Wille, V.; Rahman, M. M.; Schindler, R. N. *Ber. Bunsen-Ges. Phys. Chem.* **1991**, *95*, 1173.

(10) Paltenghi, R.; Ogryzlo, E. A.; Bayes, K. D. *J. Phys. Chem.* **1984**, *88*, 2595.

(11) Seeley, J. V.; Jayne, J. T.; Molina, M. J. *Int. J. Chem. Kinet.* **1993**, *25*, 571.

(12) Harding, L. B.; Klippenstein, S. J. Private communication, 1998.

(13) Tsang, W.; Herron, J. T. *J. Phys. Chem. Ref. Data* **1991**, *20*, 609.

(14) Biggs, P.; Canosa-Mas, C. E.; Fracheboud, J. M.; Parr, R. P.; Caralp, F. *J. Chem. Soc., Faraday Trans* **1993**, *89*, 4163.

(15) Seakins, P. W.; Leone, S. R. *J. Phys. Chem.* **1992**, *96*, 4478.

(16) To be published in the context of other alkyl radical + O reactions, see also the following. Hack, W.; Hoyermann, K.; Kersten, C.; Lendvay, G.; Olzmann, M.; Viskolcz, B. *Proc. Int. Symp. Gas Kinet., 15th* **1998**, p 113.

(17) Lindner, J.; Loomis, R. A.; Klaassen, J. J.; Leone, S. R. *J. Chem. Phys.* **1998**, *108*, 1944.

(18) Hoyermann, K.; Sievert, R. *17th Symposium (International) on Combustion*; The Combustion Institute: Pittsburgh, PA, 1979; p 517.

(19) Forst, W. *Theory of Unimolecular Reactions*; Academic Press: New York, 1973.

(20) Holbrook, K. A.; Pilling, M. J.; Robertson, S. H. *Unimolecular Reactions*, 2nd ed.; Wiley: Chichester, 1996.

(21) Gilbert, R. G.; Smith, S. C. *Theory of Unimolecular and Recombination Reactions*; Blackwell: Oxford, 1990.

(22) Olzmann, M.; Kraka, E.; Cremer, D.; Gutbrod, R.; Andersson, S. *J. Phys. Chem. A* **1997**, *101*, 9421.

(23) *CRC Handbook of Chemistry and Physics*, 75th ed.; CRC Press: Boca Raton, FL, 1994.

(24) Atkinson, R.; Baulch, D. L.; Cox, R. A.; Hampson, R. F., Jr.; Kerr, J. A.; Troe, J. *J. Phys. Chem. Ref. Data* **1992**, *21*, 1125.

(25) Beyer, T.; Swinehart, D. F. *Comm. Assoz. Comput. Mach.* **1973**, *16*, 379. Astholz, D. C.; Troe, J.; Wieters, W. *J. Chem. Phys.* **1979**, *70*, 5107.

(26) Baer, T.; Hase, W. L. *Unimolecular Reaction Dynamics*; Oxford University Press: New York, 1996.

(27) Radzig, A. A.; Smirnov, B. M. *Reference Data on Atoms, Molecules, and Ions*; Springer Series in Chemical Physics 31; Springer-Verlag: Berlin, 1985.

(28) Weaver, A.; Arnold, D. W.; Bradforth, S. E.; Neumark, D. M. *J. Chem. Phys.* **1991**, *94*, 1740.

(29) Ishiwata, T.; Tanaka, I.; Kawaguchi, K.; Hirota, E. *J. Chem. Phys.* **1985**, *82*, 2196.

(30) Pacansky, J.; Schrader, B. *J. Chem. Phys.* **1983**, *78*, 1033.

(31) Hase, W. L.; Schlegel, H. B. *J. Phys. Chem.* **1982**, *86*, 3901.

(32) Marcus, R. A.; Rice, O. K. *J. Phys. Colloid Chem.* **1951**, *55*, 894. Marcus, R. A. *J. Chem. Phys.* **1952**, *20*, 359.

(33) Frisch, M. J.; Trucks, G. W.; Head-Gordon, M.; Gill, P. M. W.; Wong, M. W.; Foresman, J. B.; Johnson, B. G.; Schlegel, H. B.; Robb, M. A.; Replogle, E. S.; Gomperts, R.; Andres, J. L.; Raghavachari, K.; Binkley, J. S.; Gonzalez, C.; Martin, R. L.; Fox, D. J.; Defrees, D. J.; Baker, J.; Stewart, J. J. P.; Pople, J. A. *Gaussian 92*, revision E.1; Gaussian Inc.: Pittsburgh, PA, 1992.

(34) Pople, J. A.; Scott, A. P.; Wong, M. W. *Isr. J. Chem.* **1993**, *33*, 345. Scott, A. P.; Radom, L. *J. Phys. Chem.* **1996**, *100*, 16502.

(35) Caralp, F.; Devolder, P.; Fittschen, C.; Gomez, N.; Hippler, H.; Méreau, R.; Rayez, M. T.; Striebel, F.; Viskolcz, B. To be published.

(36) Baulch, D. L.; Cobos, C. J.; Cox, R. A.; Esser, C.; Frank, P.; Just, Th.; Kerr, J. A.; Pilling, M. J.; Troe, J.; Walker, R. W.; Warnatz, J. *J. Phys. Chem. Ref. Data* **1992**, *21*, 411.

(37) Baulch, D. L.; Campbell, I. M.; Chappel, J. M. *J. Chem. Soc., Faraday Trans. 1* **1984**, *80*, 617.

(38) Park, J.-Y.; Gutman, D. *J. Phys. Chem.* **1983**, *87*, 1844.

(39) Frost, M. J.; Smith, I. W. M. *J. Chem. Soc., Faraday Trans.* **1990**, *86*, 1751.

(40) Pechukas, P.; Light, J. C. *J. Chem. Phys.* **1965**, *42*, 3281.

(41) Olzmann, M. *Ber. Bunsen-Ges. Phys. Chem.* **1997**, *101*, 533.

(42) Troe, J. *J. Chem. Phys.* **1983**, *79*, 6017.

(43) Schott, R.; Schlütter, J.; Olzmann, M.; Kleinermanns, K. *J. Chem. Phys.* **1995**, *102*, 8371. Ziemer, H.; Dóbé, S.; Wagner, H. Gg.; Olzmann, M.; Viskolcz, B.; Temps, F. *Ber. Bunsen-Ges. Phys. Chem.* **1998**, *102*, 897.

(44) Levine, R. D.; Bernstein, R. B. *Molecular Reaction Dynamics and Chemical Reactivity*; Oxford University Press: New York, 1987.

(45) Olzmann, M.; Gebhardt, J.; Scherzer, K. *Int. J. Chem. Kinet.* **1991**, *23*, 825.

(46) Oref, I.; Tardy, D. C. *Chem. Rev.* **1990**, *90*, 1407.

(47) Batt, L. *Int. J. Chem. Kinet.* **1979**, *11*, 977.

(48) Baldwin, A. C.; Barker, J. R.; Golden, D. M.; Hendry, D. G. *J. Phys. Chem.* **1977**, *81*, 2483.

(49) Batt, L. *Int. Rev. Phys. Chem.* **1987**, *6*, 53.

(50) Batt, L.; Milne, R. T. *Int. J. Chem. Kinet.* **1977**, *9*, 549.